Current Biology

Supplemental Information

Evolutionary Trade-Off between Vocal Tract and Testes Dimensions in Howler Monkeys

Jacob C. Dunn, Lauren B. Halenar, Thomas G. Davies, Jurgi Cristobal-Azkarate, David Reby, Dan Sykes, Sabine Dengg, W. Tecumseh Fitch, and Leslie A. Knapp

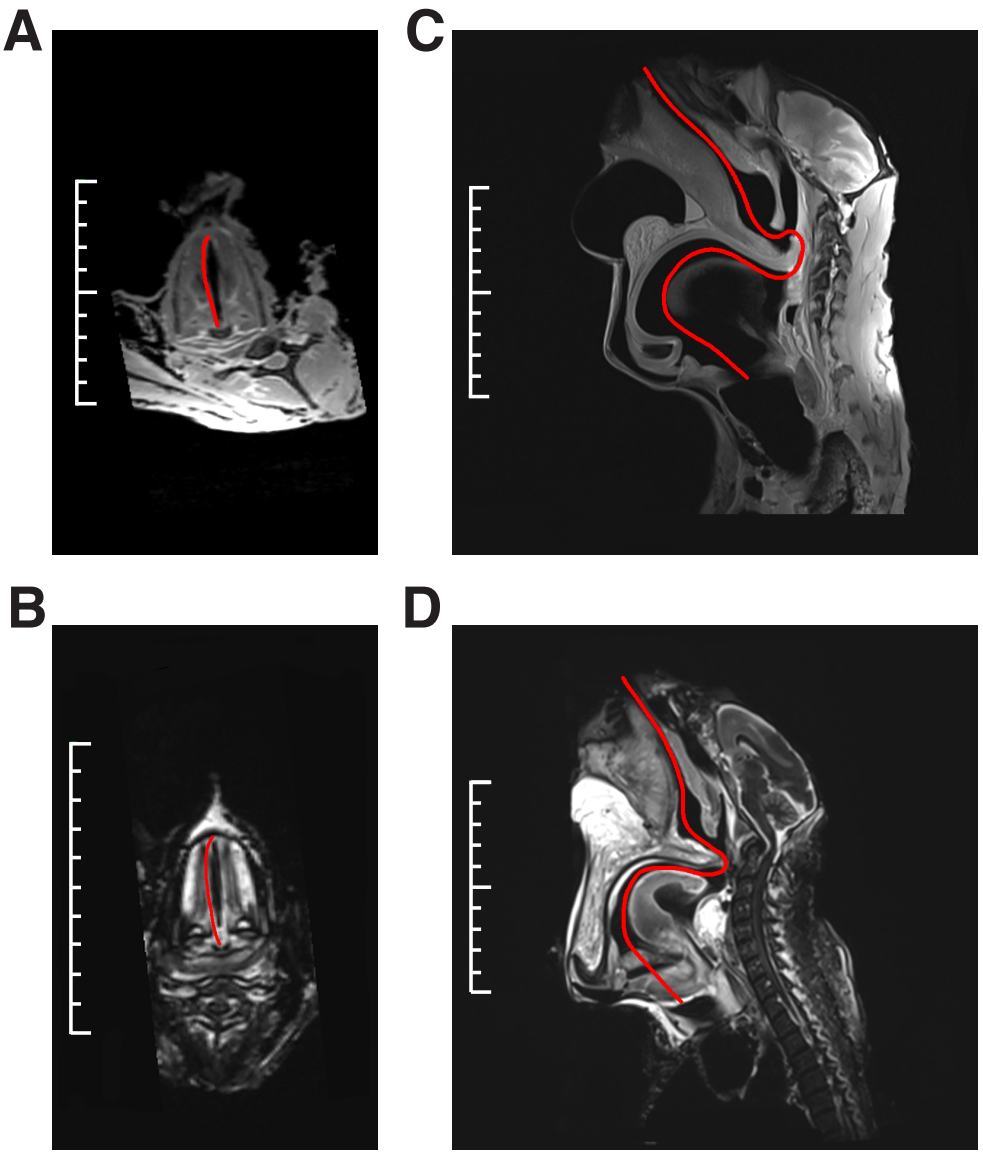

Figure S1, related to Figure 4B**.** Magnetic resonance imaging of two adult male howler monkeys. Panel (**A**) and panel (**B**) show transverse plane images of vocal fold length (traced in red) in *Alouatta sara* and *Alouatta caraya*, respectively; panel (**C**) and panel (**D**) show saggital plane images of vocal tract length (traced in red) in *Alouatta sara* and *Alouatta caraya*, respectively. The white scale on the left hand side of the images is in centimetres.

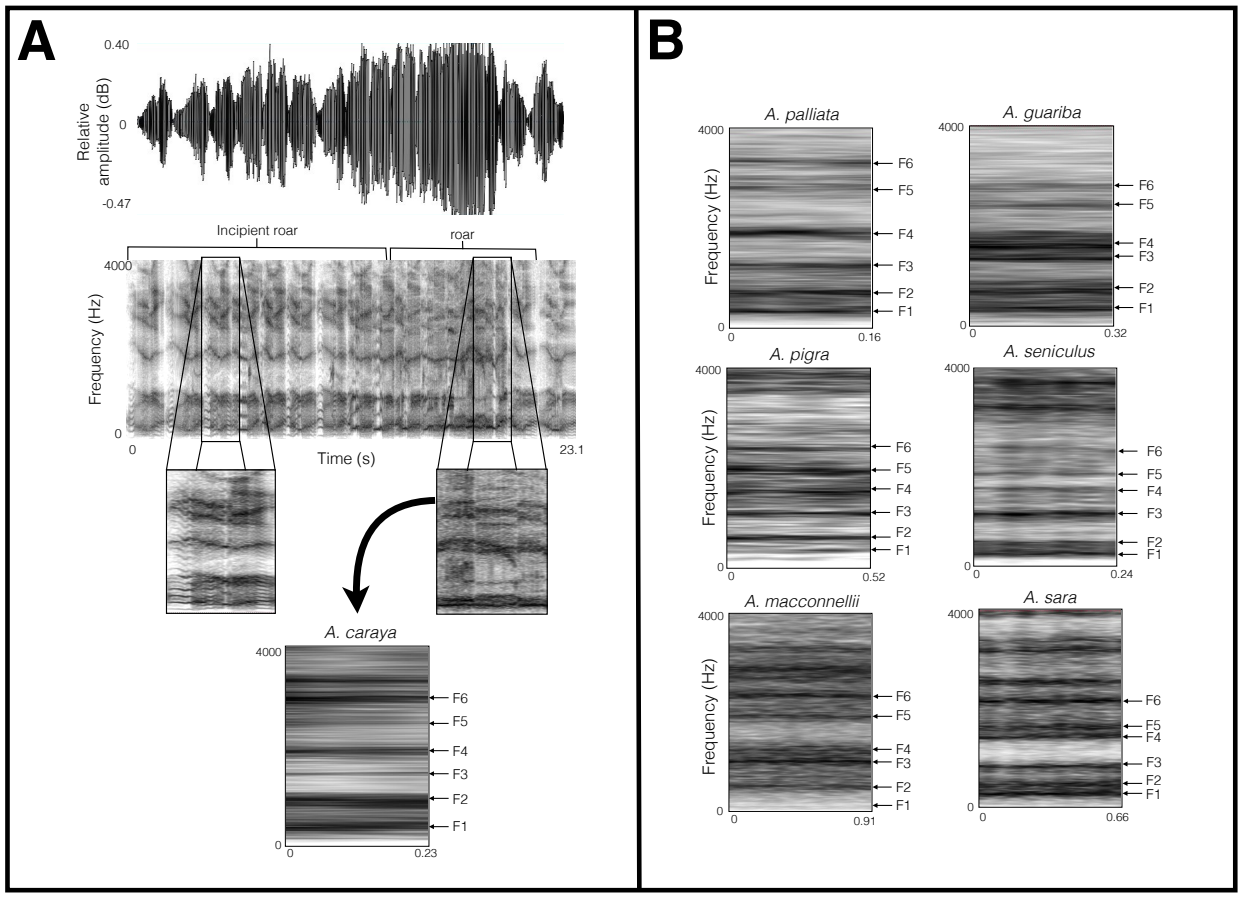

Figure S2, related to Figure 3D**. A)** Waveform (top) and spectrogram (bottom) of the vocalisations of a male howler monkey (*Alouatta caraya*). In the left hand box (incipient roar), F0 is approximately 50Hz. However, in the right hand box (roar), F0 is no longer measureable; **B)** Spectrograms of loud calls by male howler monkeys. The formants are labelled F 1 – 6.

Species	***A. belzebul***	***A. caraya***	***A. guariba***	***A. macconnellii***	***A. nigerrima***	***A. palliata***	***A. pigra***	***A. sara***	***A. seniculus***
Social organisation									
Group size	7.4 ± 1.1	9.8 ± 2.1	6.2 ± 1.1	5.9 ± 1.3	-	14.8 ± 4.4	6.8 ± 1.3	4.0 ± 1.4	7.2 ± 1.2
Number of males	1.1 ± 0.1	2.0 ± 0.4	1.4 ± 0.7	1.0 ± 0.0	-	3.0 ± 0.5	2.1 ± 0.6	1.2 ± 0.3	1.6 ± 0.4
Number of females	2.4 ± 0.5	3.2 ± 1.0	2.1 ± 0.7	1.4 ± 0.6	-	6.7 ± 2.1	2.1 ± 0.4	2.3 ± 0.4	2.3 ± 0.5
Number of sites	5	12	11	2	-	9	6	2	6
Number of groups	13	117	78	6	-	342	142	180	55
Male weight (kg)*	7.3	6.4	6.7	7.6	-	5.8	7.6	-	6.7
Female weight (kg)*	5.5	4.3	4.6	5	-	4.4	5.7	-	5.2
Male skull length (mm)	-	124.4 ± 6.8 (18)	121.31 (1)	131.2 ± 3.3 (14)	119.8 ± 6.8 (7)	-	-	130.6 ± 3.9 (8)	124.1 ± 9.2 (20)
Female skull length (mm)	-	105.1 ± 1.7 (19)	-	109.6 ± 2.7 (4)	103.9 ± 0.2 (3)	-	-	107.5 ± 3.4 (9)	108.5 ± 4.2 (14)
Male canine length (mm)*	12.3 ± 1.6 (10)	14.2 ± 2.2 (10)	14.0 ± 1.6 (7)	15.5 ± 1.0 (13)	15.3 ± 0.9 (5)	14.0 ± 2.9 (13)	13.9 ± 2.0 (6)	14.5 ± 0.4 (6)	13.4 ± 1.7 (22)
Female canine length (mm)*	6.8 ± 1.3 (9)	9.6 ± 1.4 (9)	7.8 ± 1.4 (10)	9.2 ± 0.7 (5)	8.4 ± 0.5 (4)	8.6 ± 1.4 (20)	9.6 ± 1.0 (9)	9.2 ± 0.6 (4)	9.2 ± 1.1 (18)
Male hyoid Vol. (cm^3)	53.2 ± 8.0 (3)	26.9 ± 6.0 (27)	47.0 ± 12.0 (19)	110.7 ± 22.9 (23)	61.3 ± 19.1 (9)	7.8 ± 1.3 (6)	55.1 (1)	60.5 ± 11.5 (8)	64.8 ± 14.1 (48)
Female hyoid Vol. (cm^3)	14.1 ± 3.6 (5)	8.6 ± 1.5 (25)	9.7 ± 1.4 (11)	18.5 ± 10.2 (7)	12.7 ± 2.6 (7)	2.0 ± 0.6 (4)	-	10.4 ± 1.4 (9)	14.0 ± 2.9 (43)
Testes Volume (cm^3)	-	16.7 ± 2.9 (6)	8.3 ± 3.1 (16)	-	-	22.7 ± 10.9 (24)	11.3 ± 3.8 (36)	-	3.5 ± 0.6 (5)
Formant spacing (Hz)	-	535 ± 25.9	477.7 ± 45.6	393.3 ± 10.4	-	580.7 ± 18.6	445.1 ± 5.5	387.7 ± 3.8	417.5 ± 7.8

Table S1, related to Figure 3**.** Comparative data on howler monkey social organisation, morphology and acoustics. Mean values are reported ± SD and sample sizes are given in parentheses. *For sources of data see Supplemental Experimental Procedures.

Species	Call	F1 (Hz)	F2 (Hz)	F3 (Hz)	F4 (Hz)	F5 (Hz)	F6 (Hz)	ΔF (Hz)	VTL (cm)
A. pigra	A	340	717	1255	1635	1932	2426	449.6	38.9
A. pigra	B	321	720	1250	1488	1900	2412	439.0	39.9
A. pigra	C	367	737	1199	1594	1952	2418	446.8	39.2
A. caraya	A	401	998	1418	1918	2278	2542	506.1	34.6
A. caraya	B	434	916	1488	1928	2540	2966	556.0	31.5
A. caraya	C	398	907	1381	1898	2501	2906	543.0	32.2
A. guariba	A	426	746	1415	1625	2220	2425	474.0	36.9
A. guariba	B	390	586	1218	1486	1750	2520	434.0	40.3
A. guariba	C	410	802	1402	1694	2487	2824	525.0	33.3
A. seniculus	A	314	530	1080	1571	1924	2122	412.0	42.5
A. seniculus	B	312	530	1080	1465	1920	2337	423.0	41.4
A. macconnellii	A	65	516	744	1010	1914	2326	386.0	45.3
A. macconnellii	B	63	467	981	1250	1909	2346	406.0	43.1
A. macconnellii	C	69	498	789	1006	1930	2337	389.0	45.0
A. sara	A	371	530	878	1518	1672	2186	392.0	44.6
A. sara	B	379	515	855	1500	1636	2155	386.0	45.3
A. sara	C	380	523	827	1510	1688	2108	385.0	45.5
A. palliata	A	358	712	1573	1916	2811	3340	600.0	29.2
A. palliata	B	380	748	1244	1745	2528	3340	563.0	31.1
A. palliata	C	380	754	1497	1871	2539	3340	579.0	30.2

Table S2, related to Figure 3D**.** Frequency of the first six formants, formants spacing (ΔF) and apparent vocal tract length (VTL) in the three roars analysed per species.

Species	Study Site	Gr.	M	F	N	Ref.
Alouatta belzebul	Cauaxi Ranch, Para, Brazil	6.0	1.0	2.0	1	[S1]
Alouatta belzebul	Ferreira Penna Scientific Station, Para, Brazil	9.0	1.0	3.0	1	[S2]
Alouatta belzebul	Ilha de Germoplasma, Para, Brasil	7.8	1.2	2.6	5	[S3]
Alouatta belzebul	Paranaita, Mato Grosso, Brazil	7.0	1.0	2.0	1	[S4]
Alouatta belzebul	Sapé, Paraíba, Brazil	7.4	1.2	—	5	[S5]
Alouatta caraya	Brasilera Island, Chaco, Argentina	10.9	1.8	3.4	14	[S6–9]
Alouatta caraya	Carioca Island, Upper Paraná River, Brazil	10.5	2.5	4.0	2	[S10]
Alouatta caraya	Cerro dos Negros, Rio Grande do Sul, Brazil	8.4	1.6	2.4	8	[S11]
Alouatta caraya	Corrientes Biological Field Station, Corrientes, Argentina	6.8	1.5	2.5	11	[S7]
Alouatta caraya	Guaycolec Ranch, Formosa, Argentina	7.5	1.3	1.9	15	[S12]
Alouatta caraya	Isla Guascára, Corrientes, Argentina	10.2	2.7	3.8	11	[S13]
Alouatta caraya	Mutum Island, Upper Paraná River, Brazil	10.5	2.5	5.0	2	[S10]
Alouatta caraya	Nhumirim Farm, Mato Grosso do Sul, Brazil	14.0	2.0	2.0	1	[S14]
Alouatta caraya	Porto Rico Island, Upper Paraná River, Brazil	11.0	2.0	3.0	1	[S10]
Alouatta caraya	Río Riachuelo, Corrientes, Argentina	7.2	1.6	2.3	46	[S13, S15]
Alouatta caraya	Upper Parana River (left bank), Upper Paraná River, Brazil	9.7	2.0	3.7	3	[S10]
Alouatta caraya	Upper Parana River (right bank), Upper Paraná River, Brazil	11.3	2.0	4.3	3	[S10]
Alouatta guariba	Beco Xavier, Alegrete, Rio Grande do Sul, Brazil	5.0	1.0	1.0	1	[S16]
Alouatta guariba	Campo de Instrução de Santa Maria, Rio Grande do Sul, Brazil	8.0	1.0	2.7	5	[S17]
Alouatta guariba	Cantareira Reserve, São Paulo, Brazil	5.9	1.8	2.4	26	[S18, S19]
Alouatta guariba	Chácara Payquerê, Paraná, Brazil	4.6	1.0	2.0	7	[S20]
Alouatta guariba	El Piñalito Provincial Park, Misiones, Argentina	7.5	1.0	3.0	4	[S21]
Alouatta guariba	Estação Biológica Caratinga, Minas Gerais, Brazil	6.9	1.2	2.2	29	[S22, S23]
Alouatta guariba	Fazenda Barreiro Rico, Sáo Paulo, Brazil	6.0	1.0	2.0	1	[S24]
Alouatta guariba	Intervales State Park, Sao Paulo, Brazil	5.0	2.0	1.0	1	[S25]
Alouatta guariba	Parque Estadual de Itapuã, Viamao, Rio Grande do Sol, Brazil	6.0	1.0	2.0	1	[S26]
Alouatta guariba	Porto Alegre, Viamao, Rio Grande do Sol, Brazil	7.5	3.0	3.0	2	[S27]
Alouatta guariba	Santa Genebra Reserve, Campinas, Sao Paulo, Brazil	6.0	1.0	2.0	1	[S28]
Alouatta macconnelli	Anakoko Island, Venezuela	5.0	1.0	1.0	1	[S29]
Alouatta macconnelli	Nouragues Station, French Guiana	6.8	1.0	1.8	5	[S30–32]
Alouatta palliata	Barro Colorado Island, Panama	19.7	3.2	8.6	73	[S33, S34]
Alouatta palliata	Cabo Blanco Absolute Natural Reserve, Puntarenas, Costa Rica	14.9	2.5	7.8	8	[S35, S36]
Alouatta palliata	Finca Taboga, Guanacaste, Costa Rica	11.5	2.4	5.5	22	[S37]
Alouatta palliata	Guanacaste, Costa Rica	21.8	3.1	10.2	11	[S38]
Alouatta palliata	Hacienda la Pacifica, Guanacaste, Costa Rica	12.7	2.1	6.6	92	[S39–41]
Alouatta palliata	Inland lowland forest, Chiriqui, Panama	18.9	3.9	8.0	8	[S42]
Alouatta palliata	La Selva Biological Reserve, Heredia, Costa Rica	11.0	3.3	4.0	7	[S43]
Alouatta palliata	Los Tuxtlas, Veracruz, Mexico	9.1	3.0	4.1	17	[S44, S45]
Alouatta palliata	Santa Rosa National, Park, Guanacaste, Costa Rica	13.8	3.1	5.7	104	[S46–49]
Alouatta pigra	Bermuda Landing, Gulf Coast, Belize	5.4	1.3	1.6	22	[S50, S51]
Alouatta pigra	Calakmul, Campeche Mexico	7.5	2.5	2.2	8	[S52]
Alouatta pigra	Community Baboon Sanctuary, Gulf Coast, Belize	5.9	1.5	2.0	74	[S53, S54]

Alouatta pigra	Palenque, Chiapas, Mexico	7.0	2.0	1.9	20	[S55]
Alouatta pigra	Tikal National Park, Guatemala	8.7	2.2	2.9	10	[S52]
Alouatta pigra	Yaxchilán, Chiapas, Mexico	6.6	2.8	2.0	8	[S52, S55]
Alouatta sara	Madidi National Park, Bolivia	5.0	1.4	2.5	162	[S56]
Alouatta sara	Noel Kempff Mercado National Park, Bolivia	3.0	1.0	2.0	18	[S57]
Alouatta seniculus	Estación Biológica Caparú, Vaupés, Colombia	7.0	1.0	2.0	1	[S58]
Alouatta seniculus	Finca Merenberg, Huila, Colombia	9.0	2.0	2.5	2	[S59]
Alouatta seniculus	Hato el Frio, Apure, Venezuela	7.6	1.8	3.0	5	[S60]
Alouatta seniculus	La Macarena National Park, Meta, Colombia	7.5	1.5	2.5	8	[S61]
Alouatta seniculus	Río Peneya, Meta, Colombia	5.5	1.2	1.6	29	[S62]
Alouatta seniculus	Ríos Tuparro and Tomo, Vichada, Colombia	6.3	1.9	2.4	10	[S63]

Table S3, related to Experimental Procedures**.** Review of group size and composition for study species

Dependent	Independent	Branch Lengths Normal				Branch Lengths = 1				Average No. of males			
		R^2	λ	F	P	R^2	λ	F	P	R^2	λ	F	P
Male Hy. Vol.	Female Hy. Vol.	**0.94**	**0.00**	**97.17**	**<0.001**	**0.94**	**0.00**	**97.17**	**<0.001**	**0.94**	**0.00**	**97.17**	**<0.001**
Male Can. L.	Male Body Wt.	0.00	0.00	0.00	0.95	0.00	0.00	0.00	0.96	0.00	0.00	0.00	0.95
Female Can. L.	Female Body Wt.	0.06	1.00	0.33	0.59	0.06	1.00	0.33	0.59	0.06	1.00	0.33	0.59
Male Can. L.	No. of Males	0.00	0.00	0.00	0.99	0.00	0.00	0.00	0.99	0.00	1.00	0.00	0.98
Female Can. L.	No. of Males	0.08	1.00	0.51	0.50	0.08	0.00	0.51	0.50	0.06	1.00	0.40	0.55
Male Can. L.	Male Hy. Vol.	0.15	0.00	1.07	0.34	0.05	0.00	0.31	0.60	0.15	0.00	1.07	0.34
Female Can. L.	Female Hy. Vol.	0.00	1.00	0.01	0.95	0.01	1.00	0.08	0.78	0.00	1.00	0.01	0.95
Male Can. L.	Testes Vol.	0.52	0.00	3.22	0.17	0.52	0.00	3.22	0.17	0.52	0.00	3.22	0.17
Male Hy. Vol.	Male Body Wt.	0.06	1.00	0.25	0.65	0.06	1.00	0.25	0.65	0.06	1.00	0.25	0.65
Female Hy. Vol.	Female Body Wt.	0.00	0.69	0.02	0.90	0.00	0.69	0.02	0.91	0.00	0.69	0.02	0.90
Male Hy. Vol.	No. of Males	**0.91**	**1.00**	**54.18**	**<0.001**	**0.92**	**0**	**54.18**	**<0.001**	**0.91**	**0.00**	**49.00**	**<0.001**
Female Hy. Vol.	No. of Males	**0.89**	**0.00**	**49.13**	**<0.001**	**0.89**	**0.00**	**49.13**	**<0.001**	**0.90**	**0.00**	**53.28**	**<0.001**
Testes Vol.	No. of Males	**0.78**	**0.00**	**10.45**	**0.05**	**0.78**	**0.00**	**10.45**	**0.05**	**0.76**	**0.00**	**9.45**	**0.05**
Male Hy. Vol.	Testes Vol.	**0.93**	**0.00**	**27.00**	**0.03**	**0.93**	**0.00**	**27.00**	**0.03**	**0.93**	**0.00**	**27.00**	**0.03**
Formant Spacing	Male Hy. Vol.	**0.88**	**0.00**	**30.36**	**0.01**	**0.88**	**0.00**	**30.36**	**0.01**	**0.88**	**0.00**	**30.36**	**0.01**

Table S4, related to Experimental Procedures and Figure 3. PGLS analyses using branch lengths equal to 1 in the phylogeny and using mean number of males from all groups (rather than mean per site). Hy. = Hyoid, Vol. = Volume, Can. = Canine, Wt. = Weight, No. = Number.

Supplemental Experimental Procedures

Hyoid species identification and volume calculation

We analysed hyoid volume for 255 (111 females and 144 males) apparently non-pathological, adult howler monkeys at a number of museums. Species were identified on the basis of geographic location of the site of provenance of the specimens. These coordinates were uploaded into the QGIS [S64] software package compared with the current distribution maps of *Alouatta* species from the IUCN Red List [S65].

Following a standardised protocol, we scanned the hyoids using either a NextEngine Desktop 3D laser surface scanner, with the software ScanStudio HD Pro Version 1.3.2, or a Minolta Vivid 910 laser surface scanner, with the software Geomagic Studio. We scanned the hyoids at the highest SD resolution, in macro mode. Scans were composed of 12 individual scan surfaces comprising a 360 degree rotation with ten viewpoints, and two single scans of the remaining uncaptured surfaces. We conducted initial scan trimming and alignment in ScanStudio HD. Subsequently we perfected the alignment of individual scan surfaces in Rapidform XOR with the Mesh Build-up Wizard, the Best-Fit Aligning function, and Accuracy Analyzer tool. Owing to the difficulty in capturing the internal surface of the hyoid with the 3D scanner, we calculated volume from the external surface. Thus, any part of the internal surface of the hyoid that had been captured was trimmed away leaving just the external surface. Next, we fused the individual scan faces using the Merge function, and converted the model to a solid mesh in order to calculate the volume. We filed any holes in the mesh (due to the state of preservation of the hyoid) manually using the Fill Holes function and used the settings that best created continuity in the curvature of the surface. Finally, we applied a "Global Re-mesh" to provide a relatively flat

closing to the posterior opening of the basihyal. We then calculated the volume of the final closed hyoids automatically in the software. Finished (closed) hyoid models were composed of between approximately 7,000 and 250,000 individual poly vertices, or 15,000 to 500,000 poly-faces.

Micro computed tomography (μCT) validation of volume calculations

In order to test the accuracy of the surface scan estimates of hyoid volume from the external surface of the hyoid, relative to the actual internal volume of the hyoid, we obtained μCT scans of a subsample of 4 hyoids. We performed μCT scanning using a Nikon Metrology HMX ST 225 at the Natural History Museum, London. We scanned the samples using a tungsten reflection target, at an accelerating voltage of 210 kV and current of 190 μA using a 500 ms exposure time (giving a scan time of 25 minutes). We used copper filters between 2.5 and 4 mm, depending upon the density of the hyoids. Filtering reduces the number of artifacts in the data usually produced by higher density material such as scattering and beam hardening. Higher density objects require greater levels of filtering. Over the course of a scan we took 3,142 projections over a 360° rotation of the specimen. The voxel size of the resulting datasets ranged from 70 – 111 μm depending upon the size of the specimen, as the resolution is determined by geometric magnification. We reconstructed the 3D volumes using the Feldkamp back-projection algorithm [S66] through CT Pro (Nikon Metrology, Tring, UK) and exported TIFF stacks using VG Studio Max (Volume Graphics GmbH, Heidelberg, Germany).

In Avizo Fire 6.3, we constructed isosurfaces of the hyoids by thresholding the scans. We imported the isosurfaces into Rapidform XOR, where we cropped away the external surface of the hyoid, leaving only the interior surface. We carried out the same procedures of hole filling

and re-meshing, as described above, to create a counterpart solid model of the internal volume of the hyoid. In the case of one hyoid, a laser scan was not possible (as the hyoid was articulated with the skeleton) and thus we used the μCT scan to create both the internal and external volume models. The results of the comparison show that the volume based on the external surface had an error of 5.1 ± 1.4% compared with the true internal volume and the volumes calculated using the two different methods were highly correlated ($R^2 = 0.99$, $P < 0.001$). The volume based on the external surface consistently overestimated the internal volume. An overestimate was expected, and thus this falls very closely within the expected bounds, and also suggests the procedures for closing the hyoid are not creating substantial variation. It can be assumed therefore that the errors in volume arising from the lower resolution laser scan approach, and in the method applied to create a solid model, are subject to ca. 5% error from true properties. However, we would expect this to be consistent across species and sexes.

Testes volume

We used new and published data to calculate mean ± SD testes volume per species. Only adult males were considered in the analyses. Given the technical and logistical challenges of gaining these data, we were only able to report testes volume for 5 species (Table S1). The published data were used from *A. pigra* [S67]*, A. palliata* [S67], and *A. caraya* [S68]. We collected new data for *A. guariba* at the Centro de Pesquisas Biológicas de Indaial, Brazil and for *A. seniculus* at Cologne Zoo, Germany and Parque Zoológico Santa Fe, Colombia. We followed the methods used by Kelaita et al [S67] to determine testicular volume. Briefly, we measured the width and length of each testicle, excluding scrotal skin folds, to the nearest millimeter using Mitutoyo Digital Calipers. We then used the following formula to calculate the volume of a prolate sphere:

$\pi LW^2/6$; where L is length and W is width. We used total testicular volume (sum of left and right testes) to account for any variability that exists between the left and right testes and to have data that are comparable to results presented in the literature.

Canine length

Raw data on canine length for *A. belzebul*, *A. caraya*, *A. guariba*, *A. palliata*, *A. pigra* and *A. seniculus* was kindly provided by J. Michael Plavcan from museum specimen. Methods used to collect these data have been reported elsewhere [S69]. Following these methods, we collected additional data on canine length for all remaining species from museum specimens and report the average length of left and right canines for males and females (Table S1).

Body weight

Data on body weight of wild males and females for each species were taken from a review of body size in primates [S70], with two exceptions. For *Alouatta pigra*, a more recent paper [S67] offered a much larger sample size, and for *Alouatta macconnellii* data were not reported in the original review, so they were taken from a more recent review paper [S71]. Data on body weight were not available for *Alouatta sara* or *Alouatta nigerrima* (Table S1).

Skull length

Where possible, we collected matching data on skull length for the hyoids analysed in the data set. We measured maximum skull length [S72] to the nearest mm using digital callipers. The sample consisted of 117 skulls with matching hyoids, representing 6 species (Table S1).

Group size and composition

We compiled data on group size and composition for each of the howler monkey species studied (Table S2). Much of the data came from a review paper [S71], but we complemented these data with as many additional studies as possible for each species (Table S4). We located additional records using Latin binomials as keywords in searches of Web of Science, Google Scholar and PrimateLit. Data on group size and composition were not available for *Alouatta nigerrima*. Given that local environmental factors, such as variations in climate and vegetation, may affect group size and composition within species, we calculated mean values per study site and then took the average across study sites (Table S2). We also ran the analyses using the mean values for all groups (rather than sites), and the results did not change (Table S5).

Net Primary Productivity (NPP)

We downloaded NPP data for 2013 from the Moderate Resolution Imaging Spectroradiometer (MODIS) on the Terra satellite launched by NASA [S73]. These data are freely available from the Numerical Terradynamic Simulation Group (NTSG) (http://www.ntsg.umt.edu). The data give an estimate of spatial variability in the amount of atmospheric carbon that is fixed by plants and, hence, a good estimate of forest productivity. Using the "Point Sampling Tool" in QGIS [S64], we calculated the annual NPP for the location of provenance of each hyoid specimen (Figure S2).

Calculation of theoretical fundamental frequency

The fundamental frequency (F0) of vocal fold vibration can be explained by using a simple piano-string model [S74]. In this model, vocal fold length is inversely and linearly related to F0

and can be approximated using the equation $F0 = (1/2L) \times (\sqrt{(\sigma/\rho)})$, where L is vocal fold length in m, σ is equal to the stress applied to the vocal folds in kPa, and ρ is the tissue density of the vocal folds, which is approximately equal to 1.02 g/cm^3 [S75, S76]. If we assume that there is no stress on the vocal folds during sound production [S74, S77, S78] and apply the equation to the vocal fold length of howler monkeys (ca. 40 mm), then we could predict that howler monkeys may produce an F0 as low as 15 Hz.

Acoustic analyses and calculation of apparent vocal tract length

We used bioacoustics methods to analyse the acoustic effect of variation in hyoid volume among male howler monkeys. We concentrated on males, because: (a) they howl more frequently than females, including vocalising in the context of male-male competition; (b) comparative acoustic data are much more widely available for males; and (c) the variation in hyoid volume is much greater among males.

We searched the Macaulay Library (www.macaulaylibrary.org) and the British Library Sounds archive (www.sounds.bl.uk) for high quality recordings of lone adult male roars. Many recordings were available and we screened over 300 for quality, but only a very small number were of high enough quality for reliable formant analyses. Therefore, we selected the highest quality recording of an adult male for each species. Given the very small level of within species variation in hyoid volume (Table S1), we considered these single recordings to be representative. From these recordings, we extracted three "roars" [S79] per recording for analysis.

The howler monkey roar is characterised by an introductory phase, which has classically been termed as an "incipient roar" [S79]. This section of the call contains some tonal segments and, as such, fundamental frequency can be measured in some high quality recordings. However,

incipient roars generally build in volume and grade into full roars, which are characterised by deterministic chaos and, therefore, lack periodicity and fundamental frequency may not be measured, even in high quality recordings (Figure S2). Therefore, though we could not routinely measure F0 in the roars of the males (because of the deterministic chaos typically present), we were able to measure F0 in other call types in order to make a general comparison with other mammals (Figure 4).

We extracted formant frequencies using the PRAAT 5.3.47 sound analysis package [S80]. The lowest frequency values of the first six formants were extracted using linear predictive coding (LPC) via the 'LPC: To Formants (Burg)' command in PRAAT. We did not attempt to measure formants higher than the sixth formant because these frequency components were often poorly defined. To measure the formants, we used the following analysis parameters: time-step, 0.01 s; maximum number of formants, 8-10; maximum formant frequencies, 3500–4000 Hz; window of analysis, 0.1 s. To check that the program was accurately tracking the frequency of formants, we compared the outputs with visual inspections of spectrograms and power spectra using cepstral smoothing at 200Hz. In order to ensure the reliability of our results, a bioacoustics expert with experience in formant analysis (D.R.) repeated the analyses blind to the species names. The results obtained by the two independent analysts were highly consistent.

The output of this analysis was transferred into a spreadsheet, and formant values were plotted against time and frequency and superimposed onto a narrow band spectrogram of each call. Spurious values were deleted, missing values were linearly interpolated and octave jumps were corrected for. For the first six formants, we then plotted the observed minimum frequency value of each formant against $(2i - 1)/2$ increments of the formants spacing, as predicted by the model of a vocal tract, approximated as a straight uniform tube closed at one end (the glottis) and

open at the other (the mouth) [S81]. Then, we fitted a linear regression line through the set of observed values, applying an intercept equal to 0 [S82]. Since $F_i = ((2i - 1)/2)\Delta F$, the slope of the regression gives the best estimate of ΔF for our vocal tract model. The frequency of each of the first six formants, for each of the 3 loud calls analysed per species, are given in Table S2. There was very little variation in ΔF across the three roars within species, so we took the average ΔF across the three roars for each species. In the final step, we deduced the estimated apparent VTL directly from the average ΔF by using the equation $VTL = C/2(\Delta F)$, where *c* (350 m/s) is the approximate speed of sound in the warm humid air of a mammalian vocal tract [S74].

Computed tomography (CT) and magnetic resonance imaging (MRI) of whole animals

We performed computed tomography (CT) and magnetic resonance imaging (MRI) on the cadavers of two adult male howler monkeys of different species (*Alouatta sara* and *A. caraya*) and one adult male spider monkey (*Ateles fusciceps*). We chose to examine the *Ateles* specimen in order to demonstrate the simple larynx and hyoid, typical of most primates, in this closely related taxon, and to highlight the fact that the *Alouatta* hyoid and larynx are highly modified, derived traits. The two howler monkey species were chosen to represent the greatest extremes of hyoid volume possible, given the available material. We carried out both CT and MRI at the University of Veterinary Medicine, Vienna.

We performed CT examination using a Somatom Emotion multislice scanner (Siemens AG, Munich, Germany). The specimens were placed in ventral recumbency, and scanned, depending on body size, with the following parameters: 110 – 130 kV, 94 – 174 effective mA and 0.75 mm thick axial slices. We used Avizo Fire 6.3 and Somaris/5 Syngo CT2009E (Siemens AG, Berlin) to generate multiplanar reconstructions and 3D surface models.

We performed MRI examination using a Magnetom Espree 1.5 Tesla Open Bore Design MR-System (Siemens AG, Erlangen, Germany) using a 4-canal Neck-Matrix-coil in combination with a 24-canal Spine-Matrix-coil (Siemens AG, Medical Solutions, Erlangen, Germany). Specimens were placed in ventral recumbency and scanned using the following sequences: T2-weighted 3D Turbo Spin Echo (TSE) [Repetition Time (TR): 1.500, Echo Time (TE): 225, Echo Train Length (ETL): 79, Band Width (BW): 476, Flip Angle: 130°, Slice Thickness (SL): 1 mm, Matrix: 256 x 250, Field of View (FoV): 250*250 mm], T1-weighted 3D Gradient Echo fast low angle shot [TR: 9.67, TE: 4.78, BW: 199, Flip Angle: 18.6, SL: 1 mm, Matrix: 512 x 512, FoV: 250*250 mm] and a Proton -weighted (PD) TSE [TR: 2.510, TE: 22, SL: 2 mm, ETL: 9, BW: 181, Flip Angle: 150, Matrix: 384 x 384, FoV: 250 x 250 mm]. In all cases the scanning-direction was sagittal. The phase encoding direction for the T2- and PD-weighted sequence was head-feet and for the T1-weighted anterior-posterior. We used Osirix v 5.8 [S83] to generate reconstructions and carry out anatomical measurements.

Data sources for body weight, vocal fold length and fundamental frequency

Data on body size and fundamental frequency (Figure 4a) were taken from Herbst et al. [S78]. Data on vocal fold length and fundamental frequency (Figure 4b) were from: rat [S84, S85], squirrel monkey [S86, S87], domestic cat [S74, S88], rhesus macaque [S75, S87], human[S74], sheep [S89], saiga antelope [S90], pig [S89, S91], red deer [S81, S92], cow [S89, S93], reindeer [S94], howler monkey – present study, Mongolian gazelle [S95–97], muskox [S98], tiger [S99, S100], elephant [S78] and the figure was adapted from [S77].

Statistical methods

We first used a general linear model to examine differences in hyoid volume and canine length between sexes, among species and the interaction between sex and species, and a one-way analysis of variance (ANOVA) to examine variation in testes volume among species. Then, to analyse the covariance between variables, while accounting for the non-independence of data points due to shared ancestry of species, we conducted phylogenetic generalised least squares (PGLS) regressions with a Brownian motion model of evolution, based on a published molecular phylogeny of howler monkeys [S101] (Figure 2). These models use maximum-likelihood methods to estimate Pagel`s lamda (λ) [S102], which can be used to assess the degree of phylogenetic signal in the PGLS and varies between 0 (phylogenetic independence) and 1 (species` traits covary in proportion to their shared ancestry). We used branch lengths and splitting dates from the published molecular phylogeny [S101]. Because *A. nigerrima* was not included in the published phylogeny, we used an additional molecular and karyotypic analysis of the genus, which shows that this species is more closely related to *A. macconnellii* than any other [S103]. We therefore positioned this species accordingly in the phylogeny for visual purposes (Figure 2a), but *A. nigerrima* was not used in any PGLS analyses. In order to account for potential error in the branch lengths used, we recalculated all of the PGLS analyses with branch lengths of 1 and the results did not change (Table S4). We present absolute hyoid volume and testes volume in the main text, as there was no correlation between either hyoid volume or testes volume and male body weight in our species level data, and, therefore, no effect of isometric scaling. When added to the models as a covariate, body weight accounted for very little variance and did not change our results (see below). The regression lines of the linear models and the regression lines of the full PGLS models had the same intercept and slope in all cases. Therefore,

only one line is presented in the figures. We $\log_{10}$-transformed variables in those cases where this improved the linearity of the relationships.

In the analyses that included the mean number of males per species, we used this variable as the independent variable and the morphological traits (i.e., hyoid volume, canine length and testes volume) as dependent variables. When analysing the relationship between testes volume and hyoid volume, ΔF and hyoid volume, and skull length and hyoid volume, we assigned hyoid volume as the dependent variable.

Where possible, we also used a more complete data set, rather than relying on average species level data. Firstly, in order to test the "environmental adaptation" hypothesis, we used general linear mixed models (GLMM) to evaluate the effect of NPP on hyoid volume using matching data for NPP and hyoid volume from all 255 hyoids. We specified species as a random factor in the model to account for the non-independence of species and tested the model including NPP against a null model (not including NPP) using ANOVA. In order to account for phylogenetic effects, we also carried out a PGLS regression using mean NPP values per species as the independent variable. Secondly, we used matching data on skull length and hyoid volume for 117 individuals, and performed a GLMM using species and sex as random factors in the model and hyoid volume as the dependent variable. We then tested this model against a null model (not including the variable skull length) using ANOVA. We performed all analyses in the statistical package R version 2.15.2 [S104].

Supplemental Results

The relationship between canine length and other traits

At the species level, canine length was not correlated with body weight (male PGLS: $R^2 = 0.00$, $\lambda = 0.00$, $F_{(1,5)} = 0.00$, $P = 0.95$; female PGLS: $R^2 = 0.06$, $\lambda = 1.00$, $F_{(1,5)} = 0.33$, $P = 0.59$), the number of males per group (male PGLS: $R^2 = 0.00$, $\lambda = 0.00$, $F_{(1,6)} = 0.00$, $P = 0.99$; female PGLS: $R^2 = 0.08$, $\lambda = 1.00$, $F_{(1,6)} = 0.51$, $P = 0.50$), hyoid volume (male PGLS: $R^2 = 0.15$, $\lambda = 0.00$, $F_{(1,6)} = 1.07$, $P = 0.34$; female PGLS: $R^2 = 0.00$, $\lambda = 1.00$, $F_{(1,7)} = 0.01$, $P = 0.95$) or testes volume (PGLS: $R^2 = 0.52$, $\lambda = 0.00$, $F_{(1,3)} = 3.22$, $P = 0.17$).

Adding body weight as a covariate

After adding body weight as a covariate, the number of males per group was still a significant predictor of $\log_{10}$ hyoid volume in both males (full PGLS model: $R^2 = 0.85$, $\lambda = 0.00$, $F_{(2,4)} = 11.25$, $P < 0.05$; number of males: estimate ± SE = -0.47 ± 0.10, $t = -4.71$, $P < 0.01$; male body weight: estimate ± SE = 0.12 ± 0.15, $t = 0.81$, $P = 0.46$) and females (full model: $R^2 = 0.92$, $\lambda = 0.00$, $F_{(2,4)} = 24.23$, $P < 0.01$; number of males: estimate ± SE = -0.44 ± 0.06, $t = -6.85$, $P < 0.005$; female body weight: estimate ± SE = -0.002 ± 0.09, $t = -0.03$, $P = 0.98$). Similarly, testes volume was still a significant predictor of hyoid volume (full PGLS model: $R^2 = 0.97$, $\lambda = 0.00$, $F_{(2,2)} = 34.55$, $P < 0.05$; testes volume: estimate ± SE = -3.02 ± 0.36, $t = -8.31$, $P = 0.01$; male body weight: estimate ± SE = -8.64 ± 5.40, $t = 1.59$, $P = 0.25$) and $\log_{10}$ male hyoid volume was still a significant predictor of formant spacing (full PGLS model: $R^2 = 0.97$, $\lambda = 0.00$, $F_{(2,3)} = 43.41$, $P < 0.01$; male hyoid volume: estimate ± SE = -172.44 ± 19.45, $t = -8.86$, $P < 0.05$; male body weight: estimate ± SE = -32.15 ± 15.03, $t = -2.13$, $P = 0.12$) after adding body weight as a covariate. Although the fixed effect of the number of males was still a significant predictor of testes volume after adding body weight as a covariate (estimate ± SE = 13.21 ± 3.06, $t = 4.3$, $P <$

0.05), the overall model was only borderline significant (full PGLS model: $R^2 = 0.91$, $\lambda = 0.00$, $F_{(1,3)} = 9.58$, $P = 0.09$) because of the small sample size and the noise introduced by body weight, which did not explain any of the variation (estimate ± SE = -6.25 ± 3.79, t = -1.65, $P = 0.24$).

Supplemental References

S1. Pinto, A. C. B., Ramos, C. A., and de Carvalho Jr., O. (2003). Activity patterns and diet of the howler monkey *Alouatta belzebul* in areas of logged and unlogged forest in Eastern Amazonia. Anim. Biodivers. Conserv. *2*, 39–49.

S2. De Souza, L. L., Ferrari, S. F., Da Costa, M. L., and Kern, D. C. (2002). Geophagy as a correlate of folivory in red-handed howler monkeys (*Alouatta belzebul*) from eastern Brazilian Amazonia. J. Chem. Ecol. *28*, 1613–21.

S3. Camargo, C. C., and Ferrari, S. F. (2007). Interactions between tayras (*Eira barbara*) and red-handed howlers (*Alouatta belzebul*) in eastern Amazonia. Primates. *48*, 147–50.

S4. Pinto, L. P., and Setz, E. Z. F. (2004). Diet of *Alouatta belzebul discolor* in an Amazonian rain forest of Northern Mato Grosso State, Brazil. Int. J. Primatol. *25*, 1197–1211.

S5. Bonvicino, C. (1989). Ecologia e comportamento de *Alouatta belzebul* (Primates, Cebidae) na Mata Atlântica. Rev. Nord. Biol. *6*, 149–179.

S6. Bravo, S. P. S., and Sallenave, A. (2003). Foraging behavior and activity patterns of *Alouatta caraya* in the northeastern Argentinean flooded forest. Int. J. Primatol. *24*, 825–846.

S7. Oklander, L. I., Kowalewski, M. M., and Corach, D. (2010). Genetic consequences of habitat fragmentation in black-and-gold howler *(Alouatta caraya)* populations from northern Argentina. Int. J. Primatol. *31*, 813–832.

S8. Pavé, R., Kowalewski, M. M., Peker, S. M., and Zunino, G. E. (2010). Preliminary study of mother-offspring conflict in black and gold howler monkeys (*Alouatta caraya*). Primates. *51*, 221–6.

S9. Pavé, R., Kowalewski, M. M., Garber, P. A., Zunino, G. E., Fernandez, V. A., and Peker, S. M. (2012). Infant mortality in black-and-gold howlers (*Alouatta caraya*) living in a flooded forest in northeastern Argentina. Int. J. Primatol. *33*, 937–957.

S10. Aguiar, L. M., Ludwig, G., and Passos, F. C. (2009). Group size and composition of black-and-gold howler monkeys (*Alouatta caraya*) on the Upper Paraná River, Southern Brazil. Primates. *50*, 74–7.

S11. Bicca-Marques, J. C., Prates, H. M., de Aguiar, F. R. C., and Jones, C. B. (2008). Survey of *Alouatta caraya*, the black-and-gold howler monkey, and *Alouatta guariba clamitans*, the brown howler monkey, in a contact zone, State of Rio Grande do Sul, Brazil: evidence for hybridization. Primates. *49*, 246–52.

S12. Juárez, C. P., Dvoskin, R., and Fernández-Duque, E. (2005). Structure and composition of wild black howler troops (*Alouatta caraya*) in gallery forests of the Argentinean Chaco. Neotrop. Primates *13*, 19.

S13. Rumiz, D. I. (1990). *Alouatta caraya*: Population density and demography in northern Argentina. Am. J. Primatol. *21*, 279–294.

S14. Da Cunha, R. G. T., and Byrne, R. (2006). Roars of black howler monkeys (*Alouatta caraya*): evidence for a function in inter-group spacing. Behaviour *143*, 1169–1199.

S15. Agoramoorthy, G., and Lohmann, R. (1999). Population and conservation status of the black-and-gold howler monkeys, *Alouatta caraya*, along the Rio Riachuelo, Argentina. Neotrop. Primates *7*, 43–44.

S16. Bicca-Marques, J. C., Muhle, C. B., Prates, H. M., Oliveira, S. G., and Calegaro-Marques, C. (2009). Habitat impoverishment and egg predation by *Alouatta caraya*. Int. J. Primatol. *30*, 743–748.

S17. Fortes, V. B., and Bicca-Marques, J. C. (2008). Abnormal pelage color in an isolated population of *Alouatta guariba clamitans* Cabrera, 1940 in South Brazil. Int. J. Primatol. *29*, 717–722.

S18. Da Silva Jr, E. . (1981). A preliminary survey of brown howler monkeys (*Alouatta fusca*) at the Catareira Reserve, Sao Paulo, Brazil. Rev. Bras. Biol. *41*, 897–909.

S19. Teixeira da Cunha, R. G., and Jalles-Filho, E. (2007). The roaring of southern brown howler monkeys (*Alouatta guariba clamitans*) as a mechanism of active defence of borders. Folia Primatol. *970*, 259–271.

S20. Miranda, J. M. D., and Passos, F. C. (2005). Composição e dinâmica de grupos de *Alouatta guariba clamitans* Cabrera (Primates, Atelidae) em Floresta Ombrófila Mista no Estado do Paraná, Brasil. Rev. Bras. Zool. *22*, 99–106.

S21. Holzmann, I., Agostini, I., and Bitetti, M. (2012). Roaring behavior of two syntopic howler species (*Alouatta caraya* and *A. guariba clamitans*): Evidence supports the mate defense hypothesis. Int. J. Primatol. *33*, 338–355.

S22. Mendes, S. L. (1989). Estudo ecologico de *Alouatta fusca* (Primates: Cebidae) na Estacao Biologica de Caratinga, M.G. Rev. Nord. Biol. *6*, 71–104.

S23. Strier, K. B., Mendes, S. L., and Santos, R. R. (2001). Timing of births in sympatric brown howler monkeys (*Alouatta fusca clamitans*) and northern muriquis (*Brachyteles arachnoides hypoxanthus*). Am. J. Primatol. *55*, 87–100.

S24. Martins, M. M. (2008). Fruit diet of *Alouatta guariba* and *Brachyteles arachnoides* in Southeastern Brazil: comparison of fruit type, color, and seed size. Primates. *49*, 1–8.

S25. Steinmetz, S. (2001). Drinking by howler monkeys (*Alouatta fusca*) and its seasonality at the Intervales State Park, Sao Paulo, Brazil. Neotrop. Primates *9*, 111–112.

S26. Lopes, K. G. D., and Bicca-Marques, J. C. (2011). Extragroup copulations in *Alouatta guariba clamitans*. Neotrop. Primates *18*, 52–53.

S27. De Souza Fialho, M., and Setz, E. Z. F. (2007). Extragroup copulations among brown howler monkeys in southern Brazil. Neotrop. Primates *14*, 50–52.

S28. Chiarello, A. (1994). Diet of the brown howler monkey *Alouatta fusca* in a semi-deciduous forest fragment of southeastern Brazil. Primates *35*, 25–34.

S29. Urbani, B. (2006). A survey of primate populations in northeastern Venezuelan Guayana. Primate Conserv. *20*, 47–52.

S30. Julliot, C. (1996). Fruit choice by red howler monkeys (*Alouatta seniculus*) in a tropical rain forest. Am. J. Primatol. *282*, 261–282.

S31. Julliot, C., and Sabatier, D. (1993). Diet of the red howler monkey (*Alouatta seniculus*) in French Guiana. Int. J. Primatol. *14*, 527–550.

S32. Julliot, C. (1997). Impact of seed dispersal by red howler monkeys *Alouatta seniculus* on the seedling population in the understorey of tropical rain forest. J. Ecol. *85*, 431–440.

S33. Milton, K. (1982). Dietary quality and demographic regulation in a howler monkey population. In The ecology of a tropical forest: Seasonal rhythms and long-term changes, E. Leigh, S. A. Rands, and D. Windsor, eds. (Washington, DC), pp. 273–289.

S34. Milton, K. (1996). Effects of bot fly (*Alouattamyia baeri*) parasitism on a free-ranging howler monkey (*Alouatta palliata*) population in Panama. J. Zool. *239*, 39–63.

S35. Lippold, L. (1988). A census of primates in Cabo Blanco Absolute Nature Reserve, Costa Rica. Brenesia *29*, 101–105.

S36. Lippold, L. (1989). Primates in Cabo Blanco Absolute Nature Reserve, Costa Rica. Primate Conserv. *10*, 23–25.

S37. Heltne, P., Turner, D., and Scott, N. J. J. (1976). Comparison of census data on *Alouatta palliata* from Costa Rica and Panama. In Neotropical primates: Field studies and conservation, R. Thorington and P. Heltne, eds. (Washington D.C.: National Academy of Sciences), pp. 10–19.

S38. Jones, C. B. (1985). Reproductive patterns in mantled howler monkeys: Estrus, mate choice and copulation. Primates *26*, 130–142.

S39. Clarke, M. R., Zucker, E. L., and Scott, N. J. J. (1986). Population trends of the mantled howler groups of La Pacifia, Guanacaste, Costa Rica. Am. J. Primatol. *11*, 79–88.

S40. Clarke, M. R., and Zucker, E. L. (1994). Survey of the howling monkey population at La Pacifica: A seven-year follow-up. Int. J. Primatol. *15*, 61–73.

S41. Clarke, M. R., Collins, D. A., and Zucker, E. L. (2002). Responses to deforestation in a group of mantled howlers (*Alouatta palliata*) in Costa Rica. Int. J. Primatol. *23*, 365–381.

S42. Baldwin, J. D., and Baldwin, J. I. (1976). Primate populations in Chiriqui, Panama. In Neotropical primates: Field studies and conservation, R. Thorington and P. Heltne, eds. (Washington D.C.: National Academy of Sciences), pp. 20–31.

S43. Elizabeth, K., and Stoner, E. (1994). Population density of the mantled howler monkey (*Alouatta palliata*) at La Selva Biological Reserve, Costa Rica: A new technique to analyze census data. Biotropica *26*, 332–340.

S44. Estrada, A. (1982). Survey and census of howler monkeys (*Alouatta palliata*) in the rain forest of "Los Tuxtlas", Veracruz, Mexico. Am. J. Primatol. *2*, 363–372.

S45. Estrada, A. (1984). Resource use by howler monkeys (*Alouatta palliata*) in the rain forest of Los Tuxtlas, Veracruz, Mexico. Int. J. Primatol. *5*, 105–131.

S46. Fedigan, L. M., Fedigan, L., and Chapman, C. A. (1985). A census of *Alouatta palliata* and *Cebus capuchinus* in Santa Rosa National Park, Costa Rica. Brenesia *23*, 309–322.

S47. Fedigan, L. M. (1986). Demographic trends in the Alouatta palliata and Cebus capuchinus populations of Santa Rosa National Park, Costa Rica. In Primate Ecology and Conservation, J. Else and P. C. Lee, eds. (Cambridge University Press), pp. 285–293.

S48. Fedigan, L. M., Rose, L. M., and Avila, R. M. (1998). Growth of mantled howler groups in a regenerating Costa Rican dry forest. Int. J. Primatol. *19*, 405–432.

S49. Fedigan, L. M., and Jack, K. (2001). Neotropical primates in a regenerating Costa Rican dry forest: A comparison of howler and capuchin population patterns. Int. J. *22*, 689–713.

S50. Horwich, R. H., and Gebhard, K. (1983). Roaring rhythms in black howler monkeys (*Alouatta pigra*) of Belize. Primates *24*, 290–296.

S51. Bolin, I. (1981). (*Alouatta palliata pigra*) in Belize and Guatemala. Primates *22*, 349–360.

S52. Estrada, A., Luecke, L., Van Belle, S., Barrueta, E., and Meda, M. R. (2004). Survey of black howler (*Alouatta pigra*) and spider (*Ateles geoffroyi*) monkeys in the Mayan sites of Calakmul and Yaxchilán, Mexico and Tikal, Guatemala. Primates. *45*, 33–9.

S53. Horwich, R. H., Brockett, R. C., James, R. A., and Jones, C. B. (2001). Population growth in the Belizean black howling monkey (*Alouatta pigra*). Neotrop. Primates *9*, 1–7.

S54. Ostro, L. E. T., Silver, S. C., Koontz, F. W., Horwich, R. H., and Brockett, R. C. (2001). Shifts in social structure of black howler (*Alouatta pigra*) groups associated with natural and experimental variation in population density. Int. J. Primatol. *22*, 733–748.

S55. Estrada, A., Castellanos, L., Garcia, Y., Franco, B., Munoz, D., Ibarra, A., Rivera, A., Fuentes, E., and Jimenez, C. (2002). Survey of the black howler monkey, *Alouatta pigra*, population at the Mayan site of Palenque, Chiapas, Mexico. Primates. *43*, 51–8.

S56. Wallace, R. B. unpublished data.

S57. Wallace, R. B., Painter, R. L., and Taber, A. B. (1998). Primate diversity, habitat preferences, and population density estimates in Noel Kempff Mercado National Park, Santa Cruz Department, Bolivia. Am. J. Primatol. *46*, 197–211.

S58. Palacios, E., and Rodriguez, A. (2001). Ranging pattern and use of space in a group of red howler monkeys (*Alouatta seniculus*) in a southeastern Colombian rainforest. Am. J. Primatol. *251*, 233–251.

S59. Gaulin, S. J. C., and Gaulin, C. K. (1982). Behavioral ecology of *Alouatta seniculus* in Andean cloud forest. Int. J. *3*.

S60. Braza, F., Alvarez, F., and Azcarate, T. (1981). Behaviour of the red howler monkey (*Alouatta seniculus*) in the Llanos of Venezuela. Primates *22*, 459–473.

S61. Izawa, K., and Nishimura, A. (1988). Primate fauna at the study site La Macarena, Colombia. F. Stud. New World monkeys, La Macarena, Colomb. *1*, 5–11.

S62. Izawa, K. (1976). Group sizes and compositions of monkeys in the upper Amazon basin. Primates *17*, 367–399.

S63. Defler, T. R. (1981). The density of *Alouatta seniculus* in the eastern llanos of Colombia. Primates *22*, 564–569.

S64. QGIS Development Team, T. (2014). QGIS Geographic Information System. Open Source Geospatial Found. Proj. Available at: http://qgis.osgeo.org.

S65. IUCN (2013). The IUCN Red List of Threatened Species. Version 2013.1. Available at: http://www.iucnredlist.org/.

S66. Feldkamp, L. A. (1984). Practical cone-beam algorithm. J. Opt. Soc. Am. A *1*, 612–619.

S67. Kelaita, M., Dias, P. A. D., Aguilar-Cucurachi, M. D. S., Canales-Espinosa, D., and Cortés-Ortiz, L. (2011). Impact of intrasexual selection on sexual dimorphism and testes size in the Mexican howler monkeys *Alouatta palliata* and *A. pigra*. Am. J. Phys. Anthropol. *146*, 179–87.

S68. Moreland, R. B., Richardson, M. E., Lamberski, N., and Long, J. A. (2001). Characterizing the reproductive physiology of the male southern black howler monkey, *Alouatta caraya*. J. Androl. *22*, 395–403.

S69. Plavcan, J. M., and van Schaik, C. P. (1992). Intrasexual competition and canine dimorphism in anthropoid primates. Am. J. Phys. Anthropol. *87*, 461–77.

S70. Ford, S. M., and Davis, L. C. (1992). Systematics and body size: implications for feeding adaptations in New World monkeys. Am. J. Phys. Anthropol. *88*, 415–68.

S71. Di Fiore, A., and Campbell, C. J. (2007). The atelines: Variation in ecology, behaviour, and social organization. In Primates in perspective, C. J. Campbell., A. Fuentes., K. C. MacKinnon., M. Panger., and S. K. Bearder, eds. (New York: Oxford University Press), pp. 155–185.

S72. Fitch, W. T. (1997). Vocal tract length and formant frequency dispersion correlate with body size in rhesus macaques. J. Acoust. Soc. Am. *102*, 1213–22.

S73. Zhao, M., Heinsch, F. A., Nemani, R. R., and Running, S. W. (2005). Improvements of the MODIS terrestrial gross and net primary production global data set. Remote Sens. Environ. *95*, 164–176.

S74. Titze, I. (1994). Principles of voice production (Prentice Hall).

S75. Riede, T. (2010). Elasticity and stress relaxation of rhesus monkey (*Macaca mulatta*) vocal folds. J. Exp. Biol. *213*, 2924–32.

S76. Riede, T., and Titze, I. R. (2008). Vocal fold elasticity of the Rocky Mountain elk (*Cervus elaphus nelsoni*) - producing high fundamental frequency vocalization with a very long vocal fold. J. Exp. Biol. *211*, 2144–54.

S77. Charlton, B. D., Frey, R., McKinnon, A. J., Fritsch, G., Fitch, W. T., and Reby, D. (2013). Koalas use a novel vocal organ to produce unusually low-pitched mating calls. Curr. Biol. *23*, R1035–6.

S78. Herbst, C. T., Stoeger, A. S., Frey, R., Lohscheller, J., Titze, I. R., Gumpenberger, M., and Fitch, W. T. (2012). How low can you go? Physical production mechanism of elephant infrasonic vocalizations. Science *337*, 595–9.

S79. Baldwin, J. D., and Baldwin, J. I. (1976). Vocalizations of howler monkeys (*Alouatta palliata*) in southwestern Panama. Folia Primatol. (Basel). *26*, 81–108.

S80. Boersma, P. (2001). Praat, a system for doing phonetics by computer. Glot Int. *5*, 341–345.

S81. Reby, D., and McComb, K. (2003). Anatomical constraints generate honesty: acoustic cues to age and weight in the roars of red deer stags. Anim. Behav. *65*, 519–530.

S82. Reby, D., McComb, K., Cargnelutti, B., Darwin, C., Fitch, W. T., and Clutton-Brock, T. (2005). Red deer stags use formants as assessment cues during intrasexual agonistic interactions. Proc. Biol. Sci. *272*, 941–7.

S83. Rosset, A., Spadola, L., and Ratib, O. (2004). OsiriX: an open-source software for navigating in multidimensional DICOM images. J. Digit. Imaging *17*, 205–16.

S84. Riede, T., York, A., Furst, S., Muller, R., and Seelecke, S. (2012). Elasticity and stress relaxation of a very small vocal fold. J. Biomech. *44*, 1936–1940.

S85. Jourdan, D., Ardid, D., Chapuy, E., Le Bars, D., and Eschalier, A. (1997). Audible and ultrasonic vocalization elicited by a nociceptive stimulus in rat: relationship with respiration. J. Pharmacol. Toxicol. Methods *38*, 109–16.

S86. Brown, C. H., Alipour, F., Berry, D. A., and Montequin, D. (2003). Laryngeal biomechanics and vocal communication in the squirrel monkey (*Saimiri boliviensis*). J. Acoust. Soc. Am. *113*, 2114.

S87. Fitch, W. T., and Hauser, M. D. (1995). Vocal production in nonhuman primates. Acoustics, physiology and functional constraints on honest advertisement. Am. J. Primatol. *37*, 191–219.

S88. Turner, D., and Bateson, P. (2013). The domestic cat: the biology of its behaviour 3rd ed. D. Turner and P. Bateson, eds. (Cambridge: Cambridge University Press).

S89. Alipour, F., and Jaiswal, S. (2008). Phonatory characteristics of excised pig, sheep, and cow larynges. J. Acoust. Soc. Am. *123*, 4572–81.

S90. Frey, R., Volodin, I., and Volodina, E. (2007). A nose that roars: anatomical specializations and behavioural features of rutting male saiga. J. Anat. *211*, 717–36.

S91. Schrader, L., and Todt, D. (1998). Vocal quality is correlated with levels of stress hormones in domestic pigs. Ethology *876*, 859–876.

S92. Frey, R., Volodin, I., Volodina, E., Carranza, J., and Torres-Porras, J. (2012). Vocal anatomy, tongue protrusion behaviour and the acoustics of rutting roars in free-ranging Iberian red deer stags (*Cervus elaphus hispanicus*). J. Anat. *220*, 271–92.

S93. Kiley, M. (1972). The vocalizations of ungulates, their causation and function. Z. Tierpsychol. *31*, 171–222.

S94. Frey, R., Gebler, A., Fritsch, G., Nygrén, K., and Weissengruber, G. E. (2007). Nordic rattle: the hoarse vocalization and the inflatable laryngeal air sac of reindeer (*Rangifer tarandus*). J. Anat. *210*, 131–159.

S95. Frey, R., Gebler, A., Olson, K. a, Odonkhuu, D., Fritsch, G., Batsaikhan, N., and Stuermer, I. W. (2008). Mobile larynx in Mongolian gazelle: Retraction of the larynx during rutting barks in male Mongolian gazelle (*Procapra gutturosa*, Pallas, 1777). J. Morphol. *269*, 1223–37.

S96. Frey, R. F., and Riede, T. R. (2003). Sexual dimorphism of the larynx of the Mongolian gazelle (*Procapra gutturosa*, Pallas, 1777). Zool. Anz. *242*, 33–62.

S97. Frey, R., and Gebler, A. (2003). The highly specialized vocal tract of the male Mongolian gazelle (*Procapra gutturosa*, Pallas, 1777 - Mammalia, Bovidae). J. Anat. *203*, 451–71.

S98. Frey, R., Gebler, A., and Fritsch, G. (2006). Arctic roars - laryngeal anatomy and vocalization of the muskox (*Ovibos moschatus*, Zimmermann, 1780, Bovidae). J. Zool. *268*, 433–448.

S99. Klemuk, S. A., Riede, T., Walsh, E. J., and Titze, I. R. (2011). Adapted to roar: functional morphology of tiger and lion vocal folds. PLoS One *6*, e27029.

S100. Titze, I. R., Fitch, W. T., Hunter, E. J., Alipour, F., Montequin, D., Armstrong, D. L., McGee, J., and Walsh, E. J. (2010). Vocal power and pressure-flow relationships in excised tiger larynges. J. Exp. Biol. *213*, 3866–73.

S101. Cortés-Ortiz, L., Rodríguez-Luna, E., Sampaio, I., and Ruiz-García, M. (2003). Molecular systematics and biogeography of the Neotropical monkey genus, *Alouatta*. Mol. Phylogenet. Evol. *26*, 64–81.

S102. Pagel, M. (1999). Inferring the historical patterns of biological evolution. Nature *401*, 877–84.

S103. Bonvicino, C. R., Lemos, B., and Seuánez, H. N. (2001). Molecular phylogenetics of howler monkeys (*Alouatta*, Platyrrhini): A comparison with karyotypic data. Chromosoma *110*, 241–246.

S104. Team Development Core, R. (2008). R: A language and environment for statistical computing. R Foundation for Statistical Computing, Vienna, Austria.